

Heavy Hybrids with Constituent Gluons

Eric S. Swanson^{1,2} and Adam P. Szczepaniak³

¹ *Department of Physics, North Carolina State University, Raleigh, North Carolina 27695-8202*

² *Jefferson Laboratory, 12000 Jefferson Avenue, Newport News, VA 23606*

³ *Physics Department, Indiana University, Bloomington, Indiana 47405-4202*

Abstract

Hybrid meson energies are calculated in the static quark limit with the Dynamical Quark Model (DQM). In the DQM, transverse gluons are represented as effective constituents with a dynamically generated mass. Hybrid masses are determined within the Tamm-Dancoff approximation for the resulting relativistic Salpeter equation. The model calculation agrees quite well with recent lattice data. The successes and shortcomings of the model provide clear indications about the nature of glue at low energy.

I. INTRODUCTION

A decade of experimental signals [1] for QCD hybrids (in particular with $J^{PC} = 1^{-+}$) has culminated in the claimed observation of three such states at Brookhaven [2] in the last few months. The question of the nature of QCD hybrids has thus become topical. Furthermore, lattice gauge calculations are now at the point of accurately determining light hybrid masses. In view of these developments, it is of interest to compare models of strong (low energy) QCD with lattice data to determine their viability and to explicate and guide current experimental efforts.

It is often stated that a hybrid is a hadron consisting of valence quarks and glue. However, one must specify what is meant by the notion of valence glue for this statement to be useful. There are two broad ideas in this regard: it is some sort of string or flux tube [3,4] or it is an effective constituent confined by a bag [5,6] or potential [7–9].

As an example of the importance of choosing correct degrees of freedom, we mention the simple problem of determining the number of components of a constituent gluon. It has been suggested that a massive constituent gluon should be transverse so as to maintain consistency with Yang’s theorem [8]. However it was noted that this is inconsistent with the requirements of Lorentz invariance. This issue provides an example of the importance of determining appropriate gluonic degrees of freedom. Thus, for example, $J = 1$ glueballs are expected to exist and lattice calculations indicate that they are quite heavy (roughly 3 GeV) [12]. Such a state may not be constructed from two transverse constituent gluons (Yang’s theorem) and therefore may be expected to have a mass of roughly $3m_g \sim 3$ GeV. However massive vector gluons have no such constraint and one therefore expects them to have a mass of approximately $2m_g \sim 2$ GeV.

The nature of the appropriate effective degrees of freedom for glue can only be determined by a long process of calculation and comparison with experimental and lattice data. There are, however, a few indications that low energy glue is string-like. Perhaps the most compelling of these are lattice calculations of energy, action, or field densities between static

color sources which are reminiscent of flux tubes [10]. An intriguing clue is also provided by the spin splittings of heavy quarkonia. It is known that an effective interaction free of long range exchange spin-orbit coupling is needed to reproduce the mass splitting of the 3P_J heavy quarkonium multiplets. However, an analysis of QCD in the heavy quark limit convincingly demonstrates that obtaining such an effective potential requires that low energy glue must be string-like [11].

Alternatively, pointlike models of low energy glue have a long history, originating with MIT bag model calculations of Barnes [5] and others [6]. Horn and Mandula [7] were the first to consider a potential constituent glue model of hybrids. Their hybrids consisted of constituent quarks and pointlike, massless, spinless, and colorless glue in a nonrelativistic potential model. The confining potential was taken to be linear with a string tension given by the ratio of color Casimir operators: $b_{qg} = 9/8b_{q\bar{q}}$. The authors noted that the two body $q\bar{q}$ potential is anti-confining in the color octet channel and has a repulsive Coulomb spike at short distances. They argued that this is unphysical and hence choose to neglect this term in the interaction. It is clear that a great many simplifying assumptions have gone into the construction of this model. It is our purpose to compare a more sophisticated version of the model to lattice data to learn something about these assumptions.

In the following we employ a model field theoretic Hamiltonian of QCD. The model incorporates linear confinement at low energy and evolves into perturbative QCD at high energy. A nontrivial vacuum is used to generate constituent quark and gluon masses. The Bethe-Salpeter equation is derived for a $q\bar{q}g$ system where the quarks are static. The resulting adiabatic potential surfaces are then compared to recent lattice results. We conclude that the simple picture of glue as a pointlike constituent gluon does a surprisingly good job of describing the lattice results. However, deviations at intermediate and long distances indicate that the number of effective gluons must grow with distance, eventually producing a flux tube at long distance.

II. A CONSTITUENT GLUE MODEL OF STATIC HYBRIDS

A. The Dynamical Quark Model

The starting point for our description of hybrids is the following model Hamiltonian:

$$H = \int d\mathbf{x} \psi^\dagger(\mathbf{x}) \left[-i\vec{\alpha} \cdot \vec{\nabla} + \beta m \right] \psi(\mathbf{x}) + \frac{1}{2} \int d\mathbf{x} \left[|\mathbf{E}^A(\mathbf{x})|^2 + |\mathbf{B}^A(x)|^2 \right] + \frac{1}{2} \int d\mathbf{x} d\mathbf{y} \rho^A(\mathbf{x}) V(|\mathbf{x} - \mathbf{y}|) \rho^A(\mathbf{y}) \quad (1)$$

where the color charge density is $\rho^A(\mathbf{x}) = \psi^\dagger(\mathbf{x}) T^A \psi(\mathbf{x}) - f^{ABC} \mathbf{A}^B(\mathbf{x}) \cdot \mathbf{E}^C(\mathbf{x})$ and the potential is given by

$$V(r) = \frac{\alpha_s}{r} - \frac{2N_c b}{N_c^2 - 1} r \left(1 - e^{-\Lambda_{UV} r} \right) \quad (2)$$

and $N_c = 3$. The quark mass appearing in this Hamiltonian is the current mass. To be phenomenologically successful, constituent quark masses must be generated in some way. This may be achieved by employing a BCS vacuum Ansatz; the gap equation which follows from minimizing the vacuum energy density, $\langle \Omega | H | \Omega \rangle$, (where $|\Omega\rangle$ represents the BCS trial vacuum) gives rise to a low energy constituent quark mass of roughly 200 MeV [13]. A similar calculation in the glue sector yields a gluon dispersion relation which is well-approximated by

$$\omega(k) = \sqrt{k^2 + m_g^2 e^{-k/\kappa}} \quad (3)$$

with $m_g = 800$ MeV and $\kappa = 6.5$ GeV. One sees that a constituent gluon mass of approximately 800 MeV has been generated [14]. Hadrons are then constructed on top of the BCS vacuum $|\Omega\rangle$ by employing a basis truncation (typically Tamm Dancoff or Random Phase) and solving the resulting Bethe-Salpeter equation. This approach has been used to derive the low lying spectrum of glueballs and agrees remarkably well with lattice data [14]. It should be noted that the dynamical gluons are transverse so that Yang's theorem holds and the difficulty mentioned in the Introduction does not arise.

In the following, the parameters of the model are fixed to the $q\bar{q}$ potential derived in the lattice calculation of Juge, Kuti, and Morningstar [15] (see Fig. 3 below). The fit yields $\alpha_s = 0.29$ and $b = 0.24 \text{ GeV}^2$. The final parameter, Λ_{UV} serves as an ultraviolet cutoff on the linear confinement potential. Its value was determined in Ref. [14] by fitting the gluon condensate, and will be set at 4 GeV in the following. We shall consider the static quark limit in the remainder of this work so that quark masses (and the quark sector of the BCS vacuum) become irrelevant.

The model presented here may be considered as a simplified version of the Coulomb gauge QCD Hamiltonian where the effects of nonabelian gauge couplings have been modeled by the linear confinement term. Furthermore, second order transverse gluon exchange is suppressed by the heavy quark masses. In principle, this approach allows the elimination of the ultraviolet scale Λ_{UV} via renormalization. A method for achieving this which is appropriate for nonperturbative Hamiltonian-based calculations is described in Ref. [13].

B. Static Hybrids

In the Tamm Dancoff approximation, hybrids are constructed as $q\bar{q}g$ excitations of the BCS vacuum. For the heavy hybrids considered here, the (anti)quarks serve as static color sources (sinks) and the gluons are constituent particles as described above. We choose to work in the “diatomic molecule” basis because this facilitates comparison with the lattice results of Ref. [15]. Thus our hybrid state may be written as

$$|\vec{R} n_g; j_g \Lambda \xi\rangle = \int d\vec{k} \varphi_{n_g j_g}(k) \mathcal{D}_{\mu\Lambda}^{j_g}(\hat{R}) \mathcal{D}_{\mu\lambda'}^{j_g^*}(\hat{k}) \sqrt{\frac{2j_g+1}{4\pi}} \chi_{\lambda\lambda'}^\xi \frac{T_{ab}^A}{2} b_{\vec{R}/2,a}^\dagger d_{-\vec{R}/2,b}^\dagger a_{\vec{k},A,\lambda}^\dagger |\Omega\rangle. \quad (4)$$

Wigner rotation functions are written as \mathcal{D} in this expression, R is the distance between the $q\bar{q}$ pair, λ is the gluon polarization, and φ is the radial hybrid wavefunction in momentum space. The gluon polarization wavefunction, $\chi_{\lambda\lambda'}^\xi$ is given by $\chi_{\lambda\lambda'}^1 = \delta_{\lambda\lambda'}/\sqrt{2}$ and $\chi_{\lambda\lambda'}^{-1} = \lambda\delta_{\lambda\lambda'}/\sqrt{2}$. The two cases, $\xi = 1, -1$, represent transverse magnetic and transverse electric hybrids respectively. Finally, Λ is the projection of the gluonic angular momentum onto the

$q\bar{q}$ axis, j_g is the total spin of the gluon, and n_g labels the radial basis state. We note that employing helicity basis gluon creation operators makes this expression significantly more compact than the canonical basis.

The Salpeter equation which follows from this ansatz and the Hamiltonian in Eqn. (1) may be obtained from the following matrix element:

$$\begin{aligned}
\langle \vec{R}' n'_g; j'_g \Lambda' \xi' | H | \vec{R} n_g; j_g \Lambda \xi \rangle = & \int d\vec{k} \varphi_{n'_g j'_g}^*(k) \varphi_{n_g j_g}(k) \frac{1}{2} [\omega(k) + \frac{k^2}{\omega(k)}] \\
& + \frac{3}{8} \int \int d\vec{q} d\vec{k} \varphi_{n'_g j'_g}^*(k) \varphi_{n_g j_g}(k) V(k-q) \left[\frac{\omega(k)^2 + \omega(q)^2}{\omega(k)\omega(q)} (1 + (\hat{q} \cdot \hat{k})^2) \right] \\
& - \frac{3}{4} \int \int d\vec{q} d\vec{k} \varphi_{n'_g j'_g}^*(q) \varphi_{n_g j_g}(k) V(k-q) \left(e^{i\frac{R}{2} \cdot (k-q)} + e^{-i\frac{R}{2} \cdot (k-q)} \right) \frac{\omega(k) + \omega(q)}{\sqrt{\omega(k)\omega(q)}} \times \\
& \times \mathcal{D}_{\Lambda\lambda}^{j_g*}(\hat{k}) \mathcal{D}_{\Lambda'\sigma'}^{j'_g}(\hat{q}) \sqrt{\frac{2j_g+1}{4\pi}} \sqrt{\frac{2j'_g+1}{4\pi}} \chi_{\lambda\lambda'}^\xi \chi_{\sigma\sigma'}^{\xi'} \mathcal{D}_{\mu\lambda}^1(\hat{k}) \mathcal{D}_{\mu\sigma}^{1*}(\hat{q}) \\
& + \left(\frac{1}{6} V(R) + \frac{4}{3} V(0) \right) \mathcal{N}_{n'_g j'_g n_g j_g} \delta_{j'_g j_g} \delta_{\Lambda' \Lambda} \delta_{\xi' \xi}
\end{aligned} \tag{5}$$

An overall $\delta(\vec{R}' - \vec{R})$ is understood and $\mathcal{N}_{n'_g j'_g n_g j_g} = \int dk k^2 \varphi_{n'_g j'_g}^*(k) \varphi_{n_g j_g}(k)$ is the wavefunction normalization factor. The two extra Wigner rotation matrices arise from converting the Cartesian basis implicit in Eqn. (1) and in the expression for the color current to the helicity basis, $a_{kiA} = \epsilon_H^i(k\lambda) a_{k\lambda A} = \mathcal{D}_{m\lambda}^1(\phi, \theta, -\phi) \epsilon_C^i(m) a_{k\lambda A}$, where ϵ_C and ϵ_H are canonical and helicity polarization vectors respectively.

The first term in this expression is the gluon kinetic energy, the second is the gluon self energy, the third is the gluon potential, and the fourth is the $q\bar{q}$ potential and self energies for static quarks in a color octet. The presence of the gluon and quark self energies assures the infrared finiteness of the Salpeter equation. This appears to be a general feature of color singlet states in our approach [14].

The last task is to identify the diatomic quantum numbers used to label the states. In the Jacob-Wick convention the action of parity on glue is given by

$$P a_{\vec{k}, \lambda, A} P^\dagger = \eta_g^P e^{-2i\lambda\phi} a_{-\vec{k}, -\lambda, A} \tag{6}$$

where ϕ is the azimuthal angle of \hat{k} and $\eta_g^P = -1$ is the intrinsic gluon parity. Thus the hybrid states given in Eqn. (4) are eigenstates of gluonic parity with

$$P_g|\vec{R}n_g; j_g\Lambda\xi\rangle = \xi\eta_g^P(-)^{j_g+1}|\vec{R}n_g; j_g\Lambda\xi\rangle. \quad (7)$$

A reflection of the glue degrees of freedom through a plane containing the $q\bar{q}$ axis leaves the Hamiltonian invariant and when acting on the states it takes $\Lambda \rightarrow -\Lambda$. For $|\Lambda| > 0$ one thus has doubly degenerate states. We call this operation Y -parity and perform it by setting $\hat{r}_{q\bar{q}} = \hat{z}$ and taking $y \rightarrow -y$. This may be achieved by a parity operation followed by a rotation through π about the y -axis. The action of Y on a single transverse gluon state, $|k\lambda A\rangle = a_{k\lambda A}^\dagger|0\rangle$ is therefore given by,

$$Y|k\lambda A\rangle = e^{-i\pi J_y}P|k\lambda A\rangle = \eta_g^P e^{2i\lambda\phi}|k', -\lambda, A\rangle, \quad (8)$$

where $\vec{k}' = (k_x, -k_y, k_z)$ and for the states defined in Eq. 4,

$$Y|\vec{R}n_g; j_g\Lambda\xi\rangle = \xi\eta_g^P(-)^{\Lambda+1}|\vec{R}n_g; j_g - \Lambda\xi\rangle. \quad (9)$$

where the relations $\mathcal{D}_{\mu-\mu'}^j(k') = (-)^{2j+\mu+\mu'} e^{-2i\mu'\phi} \mathcal{D}_{-\mu\mu'}^j(k)$ and $\mathcal{D}_{\mu\mu'}^j(\hat{z}) = \delta_{\mu\mu'}$ were used.

For $\Lambda \neq 0$ the Y -diagonal states may thus be written as

$$|\vec{R}n_g; j_g|\Lambda|\xi; \eta_Y\rangle = \frac{1}{\sqrt{2}} \left(|\vec{R}n_g; j_g|\Lambda|\xi\rangle + \eta_Y |\vec{R}n_g; j_g - |\Lambda|\xi\rangle \right), \quad (10)$$

where $\eta_Y = \pm 1$ and,

$$Y|\vec{R}n_g; j_g|\Lambda|\xi; \eta_Y\rangle = \xi\eta_g^P\eta_Y(-)^{\Lambda+1}|\vec{R}n_g; j_g|\Lambda|\xi; \eta_Y\rangle. \quad (11)$$

For $\Lambda = 0$ we simply have,

$$Y|\vec{R}n_g; j_g 0\xi\rangle = -\xi\eta_g^P|\vec{R}n_g; j_g 0\xi\rangle. \quad (12)$$

To allow for an easy comparison with conventions used elsewhere, we summarize the transformation properties of $\bar{q}qg$ states under total parity, $P = P_q P_g$, and charge conjugation $C = C_q C_g$, including the quark degrees of freedom.

$$P|\vec{R}n_g; j_g|\Lambda|\xi; \eta_Y\rangle = \xi\eta_g^P\eta_{\bar{q}q}^P(-)^{j_g+1}|\vec{R}n_g; j_g|\Lambda|\xi; \eta_Y\rangle \quad (13)$$

$$C|\vec{R}n_g; j_g|\Lambda|\xi; \eta_Y\rangle = \eta_g^C\eta_{\bar{q}q}^C(-)^{S_{\bar{q}q}+1}|\vec{R}n_g; j_g|\Lambda|\xi; \eta_Y\rangle \quad (14)$$

where $\eta_{q\bar{q}}^P = \eta_{q\bar{q}}^C = \eta_g^C = -1$. The states introduced in Eq. 10 are therefore also eigenstates of combined PC , with

$$PC|\vec{R}n_g; j_g|\Lambda|\xi; \eta_Y\rangle = \xi\eta_g^P\eta_g^C(-)^{j_g+S_{q\bar{q}}}|\vec{R}n_g; j_g|\Lambda|\xi; \eta_Y\rangle \quad (15)$$

After dividing out the quark portion of PC we are left with

$$(PC)_g|\vec{R}n_g; j_g|\Lambda|\xi; \eta_Y\rangle = \xi\eta_g^P\eta_g^C(-)^{j_g+1}|\vec{R}n_g; j_g|\Lambda|\xi; \eta_Y\rangle \quad (16)$$

This agrees with the expressions derived by Horn and Mandula (Eq.(29) from Ref. [7]), Le Yaouanc et al. (Eqs.(II.11) and (II.12)) from [16]) and with Ono's results (Eq.(28) in Ref. [17]). The properties of $\bar{Q}Qg$ under PC derived here disagree however, by an overall -1, with those from Ref [6] (c.f. page 304). As we discuss below, this may have important phenomenological consequences.

C. Results

The Salpeter equation is solved by expanding the radial wavefunction in a complete basis and by diagonalizing the resulting Hamiltonian matrix. The evaluation of the matrix elements is greatly facilitated by performing the angular integrals analytically. Furthermore, we found it expedient to do the remaining numerical integrals with the potential in position space since the integrand is less oscillatory for large R in this case. The plane waves and potential were expanded in a double series of Wigner functions yielding a total of ten Wigner functions. The angular integral then evaluates to a sum over a product of six Clebsch-Gordon coefficients.

As discussed above eigenstates of the Hamiltonian may be labelled with the projection of the angular momentum onto the $q\bar{q}$ axis, the product of gluonic parity with charge conjugation, $(PC)_g$ and the Y-parity eigenvalue. For $\Lambda \neq 0$ the two Y-parity eigenstates are degenerate. States are therefore denoted by Λ_P^Y where $\Lambda = 0, 1, 2$ are denoted by Σ, Π, Δ ; $(PC)_g = \eta_g^P\eta_g^C\xi(-)^{j_g+1} = g$ or u for even or odd parity respectively; and $Y = \xi\eta_g^P\eta_Y(-)^{\Lambda+1}$

$= \pm$. The total gluonic angular momentum, j_g is not a good quantum number. We have found however, that the sum over radial basis states and gluon angular momentum saturates quickly. For example, Fig 1. shows the (approximately) exact wavefunction for Σ_g^+ with $j_g = 1$ and a variational single Gaussian orbital. The next contribution to the Σ_g^+ eigenstate has $j_g = 3$, this is shown as the dotted line in the figure. Evidently the eigenstate is dominated by the lowest gluonic angular momentum component and the single Gaussian approximation is quite accurate. This remains true for all R studied here, with the $j_g = 3$ component rising to 13% of the wavefunction for $R = 10 \text{ GeV}^{-1}$. These observations support traditional approximations made for hybrids: the use of simple Gaussian wavefunctions [19] and the truncation of the adiabatic Schrödinger equation to lowest j_g [21].

FIGURES

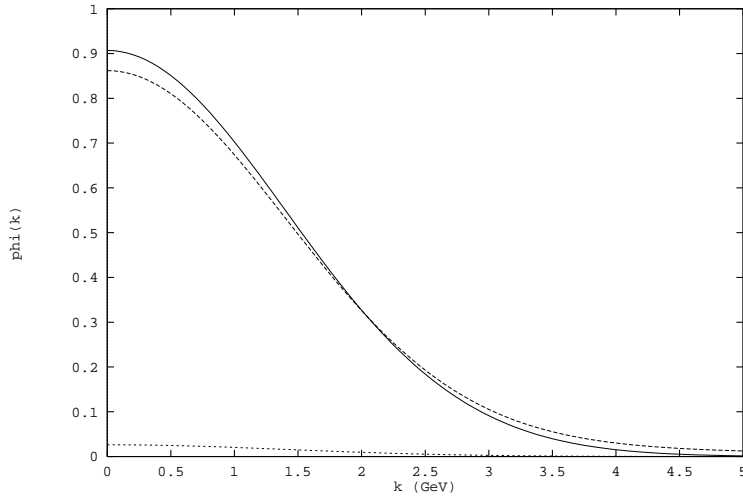


Fig. 1. Σ_g^+ wavefunctions. Exact result (dashed line), single Gaussian approximation (solid line), $j = 3$ component (dotted line).

The results for the gluon spectrum are presented as a function of the (static) quark separation in Figs. 2 and 3. They are plotted in terms of the lattice scale, $R_0 = 2.32 \text{ GeV}^{-1}$ [15] and the potentials have all been normalized by subtracting an overall constant given by $V_{q\bar{q}}(2R_0)$. In Figs. 2a-c we compare the recent lattice results from Ref. [15] with the predictions of the flux tube model [4]. The flux tube model was motivated by the strong

coupling limit of the QCD lattice Hamiltonian. It is based upon a nonrelativistic, small oscillation approximation to motion of the colored links in a topological sector where there are no overlapping (color representation of higher dimensions) or disconnected links. Since under parity (charge) conjugation the spatial (color) orientation of lattice links is reversed the nonrelativistic “beads” of the flux tube model are assumed to flip orientation with respect to the position of the quarks under parity and to have positive intrinsic charge conjugation parity.

The lowest solid line in Fig. 2a is a fit to the $q\bar{q}$ potential given by $E(R) = -4\alpha_S/(3R) + bR + \text{const}$ which corresponds to the ground state lattice Σ_g^+ potential. The other solid lines in Fig. 2 show the flux tube potential as given by

$$E(R) = bR + \frac{N\pi}{R}(1 - e^{-fb^{1/2}R}) \quad (17)$$

with $f \sim 1$ and $N = \sum_{m=1} m(n_{m+} + n_{m-})$. The latter represents the total number of right-handed (n_{m+}) and left-handed (n_{m-}) transverse phonon modes weighted by the phonon momentum (m). We note that the authors of Ref. [4] included a Coulomb term in this expression, which is incompatible with the lattice results. The flux tube model predicts the first excited $\Sigma_g'^+$ to be split by $N = 2$ from the ground states, and two degenerate Σ_u^+ and Σ_u^- potentials at $N = 3$. In the flux tube model the lowest Π state is predicted to be the Π_u . It is split from the $q\bar{q}$ ground state by $N = 1$ and is followed by the $N = 2$, Π_g potential. The two lowest Δ states, Δ_u and Δ_g correspond to $N = 2$ and $N = 3$ respectively.

The flux tube model fits the first excited state, Π_u quite well over a wide range of the quark separation and is the only surface to do so at small distance. However, we note that this may be a fluke due to the particular choice of the short distance cutoff of the π/R term employed in Ref. [4]. Alternatively, at large distances, the system is expected to act like some sort of string with an excitation energy given by π/R . The splittings do indeed appear reasonable for all the surfaces considered. It is, however, disconcerting that the Π surfaces diverge from the flux tube model predictions for $r \gtrsim 4R_0$. This must be taken as an indication that the simple flux tube model considerations fail for more complex gluonic

configurations.

In Fig.3a-c we plot the results of our calculations for Σ , Π and the Δ potentials with the flux tube results (solid lines) for comparison. While ordering of the flux tube model potentials follows the lattice data the level orderings of potentials obtained in our approach are permuted. However, they may be mapped to the lattice and flux tube ordering by simply flipping the intrinsic parity of the gluon (set $\eta_g^P = 1$ in the expressions above). In fact, this is in keeping with the assumptions of the flux tube model and with the parity of a lattice link operator (we shall discuss this further below). The resulting surfaces agree surprisingly well with the lattice results at small distances. The agreement persists to intermediate r , after which it is apparent that the model results approach the linear regime much too quickly with respect to the lattice. This is a strong indication that more degrees of freedom become active as the quark separation increases beyond $r \sim R_0 \sim 1/2$ fm. This is certainly sensible from the flux tube model point of view, where a large number of degrees of freedom are necessary to construct string phonons. Alternatively, the model presented here may be viewed as a “single bead” version (cf. Ref. [18]) of the flux tube model which is more accurate at distances comparable to the confinement length, $r \sim R_0 \sim b^{-1/2}$, than the simple flux tube model.

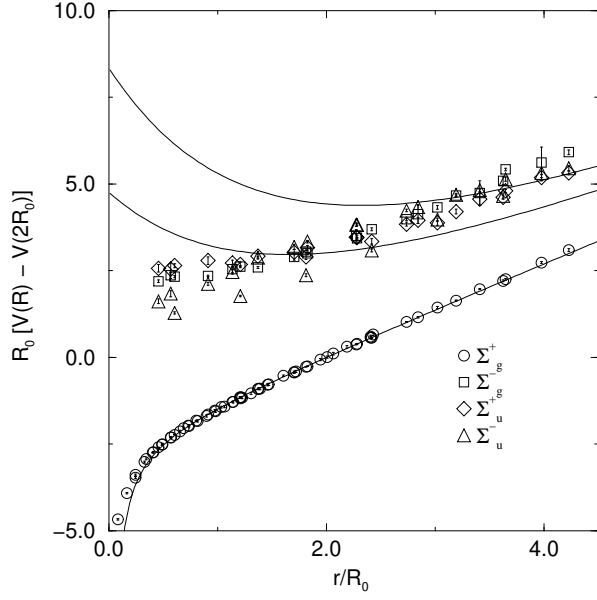


Fig. 2a. Σ surfaces. Lattice (symbols) and flux tube (lines).

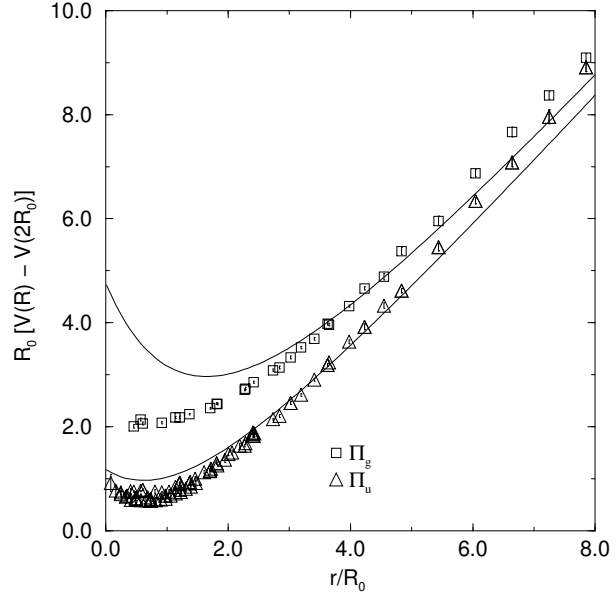


Fig. 2b. Π surfaces. Lattice (symbols) and flux tube (lines).

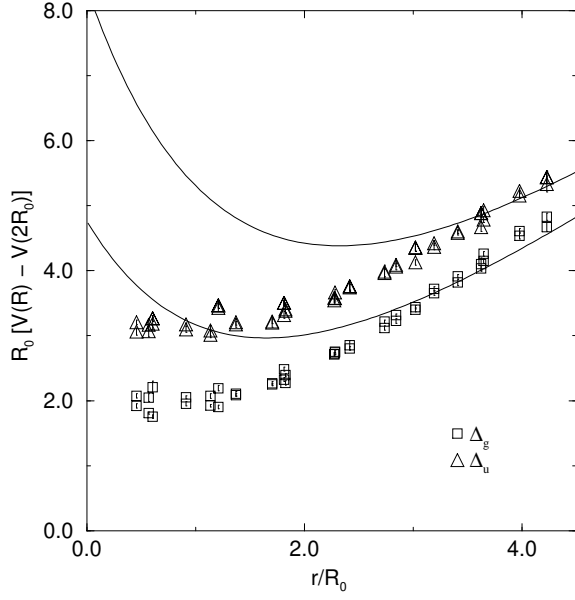


Fig. 2.c. Δ surfaces. Lattice (symbols) and flux tube (lines).

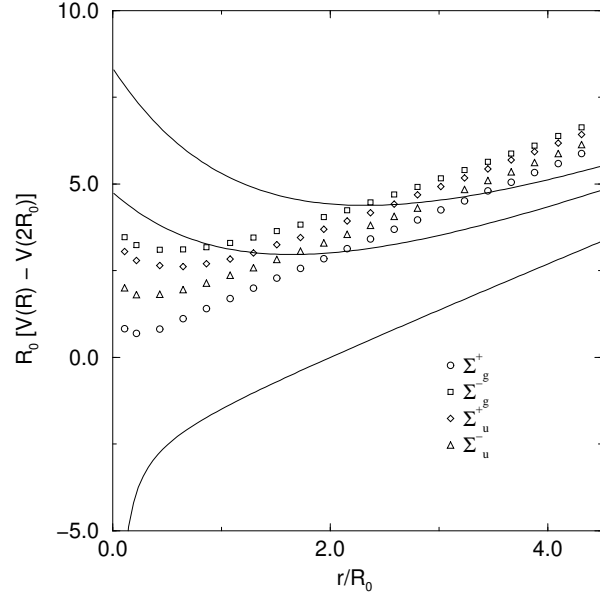


Fig. 3a. Σ surfaces. Model (symbols) and flux tube (lines).

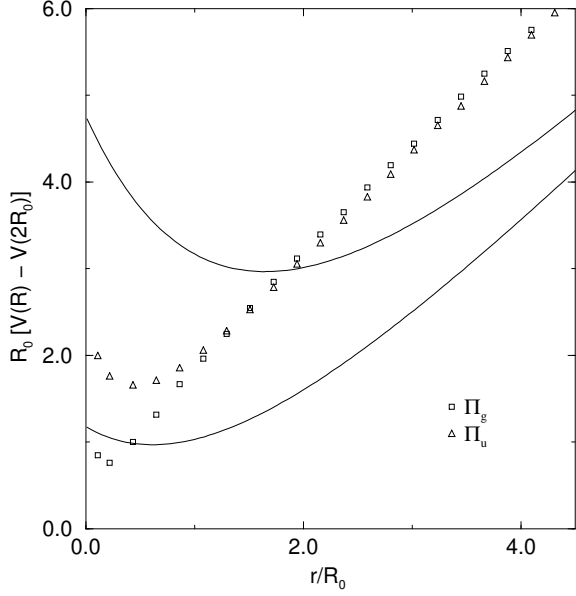


Fig. 3b. Π surfaces. Model (symbols) and flux tube (lines).

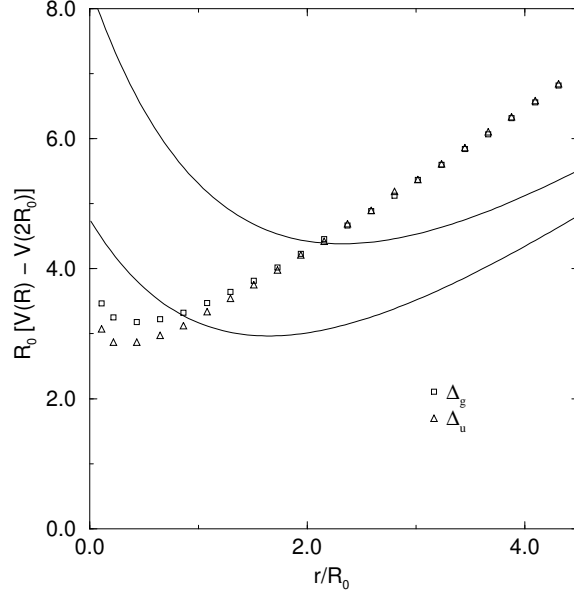


Fig. 3c. Δ surfaces. Model (symbols) and flux tube (lines).

III. CONCLUSIONS

The model presented here agrees quite well with lattice data for adiabatic hybrid potentials at short distances. However this agreement requires that the intrinsic gluon parity be taken to be positive, in keeping with the flux tube model. Thus it appears that the effective degrees of freedom describing soft glue roughly correspond to a lattice link operator, rather than to a perturbative gluon. In Ref. [21] the bag model results of [6] were compared to the same lattice calculations and the correct level ordering of potentials was found. However, as we discussed earlier, the gluonic PC given in Ref. [6] disagrees with the general derivations

given in Refs. [16,7] and the one summarized above for our model. It is therefore likely that the level orderings of both models are at odds with the lattice results. At larger distances the model becomes linear too quickly. This is a strong indication that more degrees of freedom are required to describe soft glue at large interquark separation. Indeed, one may be confident that some sort of flux tube forms at large r although the flux tube model of Ref. [4] does not seem to reproduce the Π potentials for $r \gtrsim 4R_0 \sim 2$ fm.

The results presented here include the contribution due to direct interaction between the static quarks (the last term of Eqn. (5)). This term was set to zero by Horn and Mandula [7] because it anti-confines and therefore may be expected to not produce a flux tube between the quarks. However, we note that it is responsible for producing a hybrid potential slope equal to that of the $q\bar{q}$ ground state potential, in keeping (roughly) with the lattice data. Thus we have chosen to retain this term. Note however, that this implies that there is a short distance repulsive Coulomb spike which should appear at (very) short quark separation. The appearance of this spike is, however, unphysical because the hybrid may emit a gluon and convert into a $q\bar{q}$ color singlet and a low lying glueball and this is energetically favorable for small r . Equivalently, $V_{\Pi_u} > V_{q\bar{q}} + m_{\text{gb}}$ for $r \lesssim 0.2$ fm. Thus the Coulomb spike mentioned above is irrelevant and one should see, instead, a Coulomb core for small r . This effect may be easily incorporated into the model presented here by allowing for coupling to the $q\bar{q}gg$ channel. Notice that no core is visible in the lattice data (especially in Π_u , which is measured down to $r \approx 0.04$ fm). The authors of Ref. [15] are currently examining this issue [20].

It is possible that a reasonably accurate model of soft glue may be obtained by assuming that glue is perturbative in nature at very small distances, acts as a constituent gluon (with modified parity) at intermediate distances, and evolves into a flux tube at large distance. One may imagine building such a model by allowing for a variable number of ‘gluons’ in a flux tube-type of model or by employing a bag model which has bag fluctuations as the dominant modes at large distance. The effective gluons employed in this calculation describe the lattice data reasonably well for small r and qualitatively for large r . This, coupled with

the success of the previous glueball spectrum calculation [14], indicates that the dynamical quark model provides a viable basis for calculations with glue. Several benefits of the model are particularly relevant to hybrids; light quarks may be easily incorporated, the effects of coupled channels may be examined, and the effects of light quark coupling to virtual transverse or Coulomb gluons may be included. The latter effect is of interest because it is excluded in quenched lattice calculations and may have a substantial effect on the hidden flavor hybrid spectrum.

ACKNOWLEDGMENTS

The authors are grateful to C. Morningstar for discussions and for providing us with the lattice data of Ref. [15]. This work was supported by the DOE under grants DE-FG02-96ER40944 (ES) and DE-FG02-87ER40365 (AS).

REFERENCES

- [1] D. Alde *et al.*, Phys. Lett. **B205**, 397 (1988); H. Aoyagi *et al.*, Phys. Lett. **B314**, 246 (1993); G.M. Beladidze *et al.*, Phys. Lett. **B313**, 276 (1993).
- [2] D.R. Thompson *et al.* (E852 Collaboration), Phys. Rev. Lett. **79**, 1630 (1997); A. Ostrovidov, Proceedings of Hadron 97, BNL, August, 1997.
- [3] H. Nielson and P. Oleson, Nucl. Phys. **B61**, 45 (1973); Y. Nambu, Phys. Rev. **D10**, 4262 (1974).
- [4] N. Isgur and J. Paton, Phys. Rev. **D31**, 2910 (1985).
- [5] T. Barnes, Caltech Ph.D. thesis, 1977.
- [6] P. Hasenfratz, R.R. Horgan, J. Kuti, and J.M. Richard, Phys. Lett. **95B**, 299 (1981); T. Barnes, F.E. Close, and F. De Viron, Nucl. Phys. **B224**, 241 (1983); M. Chanowitz and S. Sharpe, Nucl. Phys. **B222**, 211 (1983).
- [7] D. Horn and J. Mandula, Phys. Rev. **D17**, 898 (1978).
- [8] T. Barnes, Z. Phys. **C10**, 275 (1981).
- [9] J. Cornwall and A. Soni, Phys. Lett. **120B**, 431 (1983).
- [10] G.S. Bali, K. Schilling, and C. Schlichter, Phys. Rev. **D51**, 5165 (1995).
- [11] A.P. Szczepaniak and E.S. Swanson, Phys. Rev. **D55**, 3987 (1997).
- [12] G.S. Bali *et al.*, Phys. Lett. **B309**, 378 (1993).
- [13] A.P. Szczepaniak and E.S. Swanson, Phys. Rev. **D55**, 1578 (1997).
- [14] A.P. Szczepaniak, E.S. Swanson, C.-R. Ji, and S.R. Cotanch, Phys. Rev. Lett. **76**, 2011 (1996).
- [15] K. Juge, J. Kuti, and C.J. Morningstar, hep-lat/9709131.

- [16] A.Le Yaouanc, L. Oliver, O. Pène, J-C. Raynal, Z. Phys. C **28**, 309 (1985).
- [17] S. Ono, Z. Phys. C. **26**, 307 (1984).
- [18] T. Barnes, F.E. Close, and E.S. Swanson, Phys. Rev. **D52**, 5242 (1995).
- [19] See, for example, P. Page and F.E. Close, Nucl.Phys. **B443**, 233 (1995); E.S. Swanson and A.P. Szczepaniak, Phys. Rev. **D56**, 5692 (1997).
- [20] C.J. Morningstar, private communication.
- [21] K.J. Juge, J. Kuti, and C.J. Morningstar, hep-lat/9709132.